Heavy Neutral Leptons via Axionlike Particles at Neutrino Facilities

Asli M. Abdullahi,[1,2] André de Gouvêa,[3] Bhaskar Dutta,[4] Ian M. Shoemaker,[5] and Zahra Tabrizi[3]
[1]Instituto de Física Teórica UAM-CSIC, Universidad Autónoma de Madrid, Cantoblanco, 28049 Madrid, Spain
[2]Particle Theory Department, Fermi National Accelerator Laboratory, Batavia, Illinois 60510, USA
[3]Department of Physics and Astronomy, Northwestern University, 2145 Sheridan Road, Evanston, Illinois 60208, USA
[4]Mitchell Institute for Fundamental Physics and Astronomy, Department of Physics and Astronomy, Texas A&M University, College Station, Texas 77843, USA
[5]Center for Neutrino Physics, Department of Physics, Virginia Tech, Blacksburg, Virginia 24061, USA

(Received 7 June 2024; accepted 18 November 2024; published 24 December 2024)

Heavy neutral leptons (HNLs) are often among the hypothetical ingredients behind nonzero neutrino masses. If sufficiently light, they can be produced and detected in fixed-target-like experiments. We show that if the HNLs belong to a richer—but rather generic—dark sector, their production mechanism can deviate dramatically from expectations associated with the standard-model weak interactions. In more detail, we postulate that the dark sector contains an axionlike particle (ALP) that naturally decays into HNLs. Since ALPs mix with the pseudoscalar hadrons, the HNL flux might be predominantly associated with the production of neutral mesons (e.g., π^0, η) as opposed to charge hadrons (e.g., $\pi^\pm$, $K^\pm$). In this case, the physics responsible for HNL production and decay are not directly related and experiments like DUNE might be sensitive to HNLs that are too weakly coupled to the standard model to be produced via weak interactions, as is generically the case of HNLs that play a direct role in the type-I seesaw mechanism.

DOI: 10.1103/PhysRevLett.133.261802

Introduction—The discovery of neutrino oscillation [1–3], and the confirmation of nonzero neutrino masses, implies the existence of fields beyond those of the standard model (SM) of particle physics. While little is known about these new degrees of freedom, a plethora of extensions have been proposed to explain the origin of the neutrino mass. Many of these extensions invoke the existence of SM-singlet fermions, commonly referred to as right-handed, or sterile, neutrinos. Popular examples of such models include the type-1 seesaw mechanism [4–12] and other seesaw variants [9–16]. Depending on their properties, these singlet fermions may help shed light on other outstanding problems in particle physics, including the abundance of dark matter [17–20] and the baryon asymmetry of the Universe [21,22].

SM-singlet fermions can interact with SM particles through Yukawa interactions involving the Higgs-doublet H and the lepton doublets L, in what is known as the neutrino portal. Such a coupling induces a mixing between the active neutrinos $\nu_{e,\mu,\tau}$ and the SM-singlet fermions N_{s_j}, $j = 1, \ldots, n_s$, generating a Dirac mass for the neutrinos after electroweak symmetry breaking. The singlet fermions may or may not have a Majorana mass, although such a mass term is always permitted by symmetry. We are left with mass eigenstates ν_i, with masses m_i, that are linear superpositions of the active and singlet states, $\nu_i = U^\dagger_{\alpha i}\nu_\alpha$, where α now runs over $\alpha = e, \mu, \tau, s_1, s_2, \ldots, s_{n_s}$. The transformation is parametrized by the unitary $(3 + n_s) \times (3 + n_s)$ matrix, with components $U_{\alpha i}$. Henceforth, we will restrict our discussions to $n_s = 1$ and refer to the new fermion as N. We are interested in mass scales of order 1 MeV to 1 GeV for the new particle, a region of parameter space that has garnered particular interest in recent years as it lies within reach of a number of search programs, including fixed-target, meson decay, and collider experiments [23–29]. In this mass region, the N is often referred to as a heavy neutral lepton (HNL) and it is the $U_{\alpha 4}$ element of the mixing matrix that typically governs its production in fixed-target experiments, along with its scattering cross section in the detector and its decay properties.

The existence of SM-singlet fermions invites one to consider a richer "dark sector" with its own particle content and interactions [30–43] (see also Ref. [44] and references therein for more general dark sector models on HNLs). Generically, it is useful to allow for the possibility that N, while a SM singlet, is charged under a "dark" gauge group and interacts with other particles that are also SM singlets.

We will concentrate on dark sectors that also contain a new pseudoscalar a, with nonzero mass, sometimes referred to as an axionlike particle (ALP). We will further assume that a couples to N and that its mass is such that it

decays predominantly to pairs of HNL. This is not an especially extraordinary hypothesis as it mimics the SM. In the SM, the strong interactions confine and the lightest propagating hadronic degrees of freedom are pseudoscalars (pions, kaons, etc.). The lightest among these are restricted to decaying weakly into pairs of leptons (e.g., $\pi^+ \to \mu^+\nu$) or electromagnetically into photons (e.g., $\pi^0 \to \gamma\gamma$). If the dark sector is anything like the SM, it is easy to imagine scenarios where $a \to NN$ is similarly inevitable. A complete chiral dark sector model with these characteristics was proposed and explored in Ref. [45]. There, the ALPs were referred to as "dark pions" and the HNLs as "dark neutrinos." We will refer to Ref. [45] when discussing concrete realizations of the scenario of interest, but emphasize that our results remain general and not tied to any specific model.

In the absence of the ALP, in fixed-target-like experiments and for HNL masses below a GeV, the HNLs are typically produced in the decay of charged mesons (e.g., $\pi^+ \to \mu^+ N$). In this case, the production rate is proportional to $|U_{\alpha 4}|^2$. Further downstream, the N can be detected via its decays to SM particles, with the N partial widths also proportional to $|U_{\alpha 4}|^2$. If a kinematically accessible ALP is now added to the picture, we allow for a new HNL production mechanism in fixed-target-like experiments. The ALPs mix with *neutral* pseudoscalar mesons (π^0, η, etc.) and are produced in tandem with light hadrons at the target. This production rate is, of course, independent of $U_{\alpha 4}$. The ALPs then decay to HNL pairs with large branching ratios and HNL decays downstream can lead to an observable signal in the detector.

While generic ALP-HNL couplings have been studied in the literature, the focus has typically been on the constraint posed by experiment on the coupling itself [46,47] or the contribution to existing processes coming from such a coupling [48]. In this Letter, we focus on the impact of an ALP-HNL coupling on the discovery potential of HNLs in fixed-target-like experiments. We explore the consequences of this new HNL production mechanism at the DUNE near-detector complex, taken as a particularly relevant experimental setup. Figure 1 provides a schematic of the production-decay-detection process. We find that, depending on the ALP properties, one can explore previously inaccessible regions of the HNL parameter space, including the region preferred by the type-I seesaw model for neutrino masses.

Heavy ALP production—The ALP a is a pseudoscalar field and mixes with the SM pseudoscalar mesons, including the π^0 and the η. Following Refs. [49–51] and especially Ref. [52], the relevant mixing contributions of the SM mesons to the ALP can be defined as

$$\pi^0 \to \pi^0 + g_{\pi a} a, \tag{1}$$

$$\eta \to \eta^0 + g_{\eta a} a, \tag{2}$$

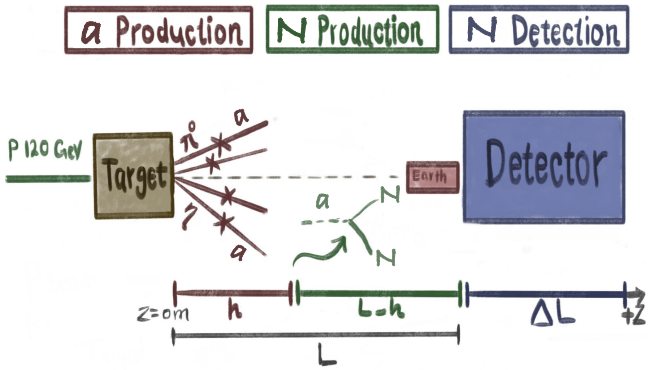

FIG. 1. Schematic description of the production of ALPs (a) followed by the production of heavy neutral leptons (N), in a fixed-target experimental setup. In the DUNE near-detector complex, a beam of 120 GeV protons impinges on a target, producing charged and neutral mesons. ALP production is proportional to that of neutral mesons: the crosses represent a-neutral-meson mixing. The ALP travels toward the detector and decays into a pair of HNLs a distance h from the target. The HNLs that reach the detector (width ΔL, a distance L from the target) may decay inside the detector volume into SM particles, yielding an observable signal. Not to scale.

where the meson mixing parameters are [52]

$$g_{\pi a} = \frac{1}{6}\frac{f_\pi}{f_a}\frac{m_a^2}{m_a^2 - m_{\pi^0}^2}, \tag{3}$$

$$g_{\eta a} = \frac{1}{\sqrt{6}}\frac{f_\pi}{f_a}\left(\frac{m_a^2 - \frac{4}{9}m_{\pi^0}^2}{m_a^2 - m_\eta^2}\right). \tag{4}$$

In order to estimate the ALP production rate at a fixed-target facility, we assume that the probability of producing an a particle with three-momentum $\vec{p}_a$ is the same as that to produce a pseudoscalar $\mathbf{m}$ with the same three-momentum, up to a scaling factor $g_{\mathbf{m}a}^2$. This is a good approximation as long as the mass of the ALP is similar to the hadronic pseudoscalar masses. With this in mind, the ALP differential flux is proportional to that of the pseudoscalar $\mathbf{m}$,

$$\frac{d^2\phi_a}{dE_a d\theta_a} = g_{\mathbf{m}a}^2 \frac{E_a}{E_\mathbf{m}}\frac{d^2\phi_\mathbf{m}}{dE_\mathbf{m} d\theta_\mathbf{m}}, \tag{5}$$

where $\phi_{a,\mathbf{m}}$ are the ALP and meson fluxes, $E_{a,\mathbf{m}}$ their respective energies, and $\theta_a = \theta_\mathbf{m}$ is the angle defined by the outgoing ALP-meson three-momentum and the direction of the incoming proton beam. For meson fluxes at the DUNE near-detector facility, assuming the SM, we used the results from Refs. [53,54], obtained with GEANT4 [55].

Integrating Eq. (5) over θ_a and E_a, Fig. 2 depicts the ALP flux as a function of the ALP mass m_a, considering the contributions from ALP-π^0 (dotted orange curve) and ALP-η (dashed blue curve) mixing. We assume a proton-on-target (POT) rate of 1.1×10^{21} per year for a period of

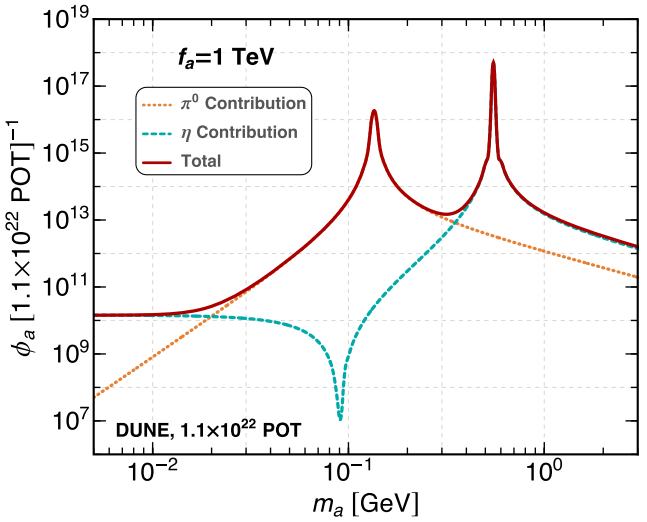

FIG. 2. Expected ALP flux at the DUNE near-detector facility as a function of the ALP mass m_a. The dotted orange (dashed blue) curve corresponds to the contribution from ALP-π^0 (ALP-η) mixing, while the total flux is depicted with the solid red curve. We assume a total exposure of 1.1×10^{22} protons on target and $f_a = 1$ TeV. The ALP flux is proportional to f_a^{-2}, see text for details.

10 yr [56] and choose $f_a = 1$ TeV. The ALP flux is proportional to f_a^{-2} [see Eqs. (3)–(5)]. We restrict the plot to m_a values under a few GeV since the mixing formalism discussed above fails for larger values of m_a.

HNL production—Once produced, we assume that the ALP decays exclusively into a pair of HNLs. For the decay rate, we use the model discussed in Ref. [45], where ALP decays into HNLs parallel the decays of charged pions into lepton pairs, mediated by W-boson exchange. The partial width is given by

$$\Gamma(a \to 2N) = \frac{1}{4\pi v_D^4} f_a^2 m_a m_N^2. \tag{6}$$

Here, v_D is the vacuum expectation value of the dark sector Higgs-like scalar and m_N is the HNL mass. Here we assume v_D to be much larger than the weak scale [45]. Like SM pion decay, $a \to 2N$ is chirality suppressed. For very small m_N values, the four-body decay $a \to 4N$ is significant or even dominant (one SM parallel to this decay mode is $\pi^0 \to Z^* Z^* \to 4\nu$). See Ref. [45] for details. Here, we restrict our discussion to regions of parameter space where the two-body final state dominates.

The probability that the ALP decays inside an infinitesimal interval Δh a distance h from the production target is

$$\left(\frac{\mathrm{d}P^a_{\mathrm{decay}}}{\mathrm{d}h}\right)\Delta h = \left(\frac{\Gamma}{(\beta\gamma)_a} e^{-\Gamma_a h/(\beta\gamma)_a}\right)\Delta h, \tag{7}$$

where Γ_a is the ALP decay width and $(\beta\gamma)_a = |\vec{p}_a|/m_a$ is the boost-velocity factor. We are interested in decays that occur before the detector, a distance L away: $0 \leqslant h \leqslant L$. In the case of DUNE, $L = 574$ m.

In the ALP rest frame, the two HNLs are produced back-to-back and the decay is, of course, isotropic. In order to compute the HNL flux, we simulate ALP decays in the lab frame and assume the detector to be a cylinder with radius r, aligned with the beam direction ("on axis"). Since the HNLs are produced at a distance h from the target (see Fig. 1), HNLs reach the detector as long as their production angles (relative to the beam direction) in the lab frame are smaller than the opening angle of the detector $\theta_{\mathrm{det}} = \arctan(r/L - h)$.

The total flux of HNLs arriving at the detector can be computed by combining the differential ALP flux and the decay rate. It is

$$\phi_N = \int \sin\theta_a \frac{d^2\phi_a}{dE_a d\theta_a} \frac{\mathrm{d}P^a_{\mathrm{decay}}}{\mathrm{d}h} dE_a d\theta_a \times \Theta(\theta_{\mathrm{det}} - \theta) P^N_{\mathrm{sur}} \frac{d\Omega}{4\pi} dh, \tag{8}$$

where $d\Omega$ and θ refer to the direction of the HNL and P^N_{sur} is the probability that an HNL reaches the detector before decaying,

$$P^N_{\mathrm{sur}} = e^{-\Gamma_N (L-h)/(\beta\gamma)_N}. \tag{9}$$

Γ_N, $(\beta\gamma)_N$ are, respectively, the decay width and boost-velocity factor of the HNL.

Figure 3 depicts the HNL flux at the detector as a function of the HNL mass m_N, for different values of f_a

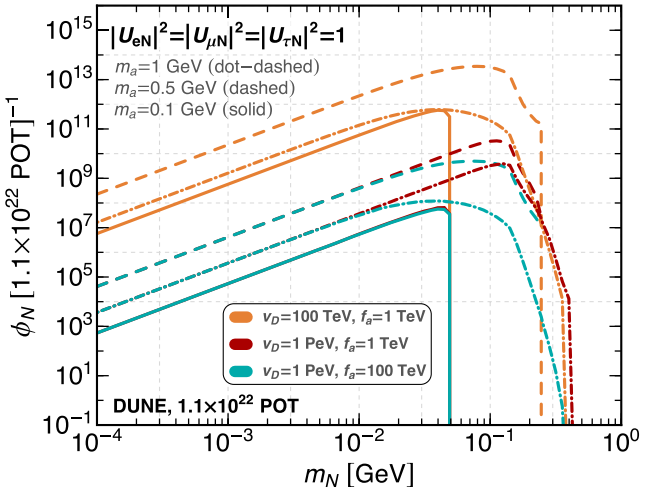

FIG. 3. HNL flux at the detector as a function of the HNL mass m_N, assuming a total exposure of 1.1×10^{22} protons on target. Different colors correspond to different values of f_a and v_D (labeled), while the solid (dashed) curves correspond to $m_a = 0.2(0.8)$ GeV.

and v_D, for $m_a = 0.2(0.8)$ GeV [solid (dashed) curves] and $|U_{\alpha 4}|^2$ equals one for all $\alpha = e, \mu, \tau$. The HNL flux gets enhanced for $m_a = 0.5$ due to the resonancelike behavior in Fig. 2. The ALP production rate is proportional to $1/f_a^2$, while the ALP decay rate into HNLs is proportional to $(f_a/v_D^2)^2 \exp -(f_a m_a m_N/v_D^2)^2 h/|p_a|$. For our choices of parameters, ALP always decays between the source and the detector.

HNL event rates—HNLs decay via SM interactions through their mixing with the active neutrinos; we assume the dark sector parameters are such that there are no other allowed decay modes. The total and partial decay widths are governed by the HNL mass m_N and the elements of the mixing matrix $U_{\alpha 4}$, $\alpha = e, \mu, \tau$ [28,45,57,58]. HNL decays inside the detector are potentially observable and constitute our signal.

For a given exposure time $\mathcal{T}$, the total event rate from HNL decays into a final state X, $N_{\rm signal}(X)$, at the detector is given by a convolution of the decay probability of the HNL into X and the HNL flux, Eq. (8),

$$N_{\rm signal}(X) = \mathcal{T} \int \sin\theta_a \frac{d^2\phi_a}{dE_a d\theta_a} \frac{{\rm d}P^a_{\rm decay}}{{\rm d}h} dE_a d\theta_a \times \Theta(\theta_{\rm det} - \theta) P^N_{\rm sur} \frac{d\Omega}{4\pi} dh \times P^N_{\rm decay} \mathcal{B}(N \to X), \quad (10)$$

where $\mathcal{B}(N \to X)$ is the branching ratio of the HNL decay into X and the probability the decay happens inside the volume of the detector, with the length ΔL, is

$$P^N_{\rm decay} = e^{-\Gamma^{\rm Total}_N (L-h)/(\beta\gamma)_N} \left[1 - e^{-\Gamma^{\rm Total}_N \Delta L/(\beta\gamma)_N}\right]. \quad (11)$$

The HNL lifetimes and the various branching fractions can be found in Appendix A of Ref. [45]; we depict different branching ratios as a function of m_N in Fig. 5 of the Appendix in the End Matter. We consider the charged-current mediated channels $X = e^\pm\pi^\mp, \mu^\pm\pi^\mp, \nu e^\pm\mu^\mp$, the neutral-current mediated channel $X\nu\pi^0$, the "mixed" channels $X = \nu\ell^+\ell^-$ ($\ell = e, \mu$), and the one-loop channel $X = \nu\gamma$. We pay special attention to $X = \nu e^+ e^-$ since it has the largest branching fraction for m_N below m_π and contributes appreciably for larger masses. At small m_N, $X = \nu\gamma$ is also of interest, even though it has a much smaller branching smaller.

DUNE analysis and results—In order to estimate the sensitivity of the DUNE near-detector facility to HNLs produced via ALP decays, we assume a cylindrical (radius $r = 2.6$ m and length $\Delta L = 10$ m), on axis, 50 ton liquid argon near detector, located $L = 574$ m from the target. We assume 10 yr of data taking with an exposure of 1.1×10^{21} POT/yr [56]. We estimate the sensitivity to the HNL parameter space using a naive χ^2 analysis based on the expected HNL rate $N_{\rm HNL}$, where for 90% confidence level and 2 degrees of freedom we use $N_{\rm HNL} = 4.61$. The model of interest contains eight assumed-to-be-uncorrelated parameters: $(f_a, v_D, m_a, m_N, |U_{\alpha 4}|^2)$, $\alpha = e, \mu, \tau$. For each final state, we perform an independent analysis and "turn on" only one $|U_{\alpha 4}|^2$ at a time (i.e., only one among $|U_{eN}|^2$, $|U_{\mu N}|^2$, and $|U_{\tau N}|^2$ are nonzero at a given analysis). Unless otherwise noted, we fix $m_{\pi_D} = 3m_N$, for concreteness.

For simplicity, we do not include backgrounds in our analyses. We expect this to be a reasonable assumption for some HNL-decay final states, including $e^+e^-\nu$, but are quite confident this is not the case for other final states, where significant beam-induced backgrounds are expected. A dedicated study is necessary for properly estimating the different backgrounds. We leave such background studies for future work.

Our results in the $m_N \times |U_{\alpha 4}|^2$ plane, for fixed $f_a = 1$ and $v_D = 10^2$ TeV are depicted in Fig. 4. The top, middle, and bottom panels correspond ν_e-coupled, ν_μ-coupled, and ν_τ-coupled HNLs, respectively. For very small $|U_{\alpha 4}|$, HNL production is severely suppressed since the HNLs are too long-lived to decay inside the detector. There are regions of enhanced sensitivity at $m_N \sim 40$ and $m_N \sim 200$ MeV. These correspond to the resonant-production peaks observed in Fig. 2 when $m_a \sim 120$ and $\sim$600 MeV, respectively. For m_N smaller than, roughly, the pion mass, only the $\nu e^+ e^-$ and $\nu\gamma$ channels are open. These remain competitive for larger values of m_N but are superseded by decay modes with larger branching ratios. Results for $v_D = 10^3$ TeV are depicted in Fig. 6 of the Appendix in the End Matter.

Regardless of whether the HNL is purely ν_e coupled (only $|U_{e4}| \neq 0$), ν_μ coupled (only $|U_{\mu 4}| \neq 0$), or ν_τ coupled (only $|U_{\tau 4}| \neq 0$), the overall sensitivities are approximately the same. This is to be contrasted with the standard scenario in which the HNLs are the product of charged-meson decays. There, due to the comparative sizes of the respective parent meson fluxes, the sensitivity to ν_μ-coupled HNLs is superior to that of ν_e-coupled HNLs, which is in turn superior to that of ν_τ-coupled HNLs. This is especially relevant for τ-coupled HNLs whose production is severely suppressed by the flux of charm mesons (e.g., D_s) at the target or, in the case of lower-energy facilities, completely absent. The enhanced production of τ-coupled HNLs makes it possible to better probe the $|U_{\tau 4}|$ coupling, as well as search for the potential detector signatures of the τ lepton [59–64].

For the ALP parameters of choice, in this Letter we are sensitive to significantly smaller $|U_{\alpha 4}|$ values. This is expected. For charged-meson-produced HNLs, the signal rate is naively proportional to $|U_{\alpha 4}|^4$, while for neutral-meson-produced HNLs, the signal rate is naively proportional to $|U_{\alpha 4}|^2$. For the scenario considered here, we find that DUNE is sensitive to HNLs whose parameters

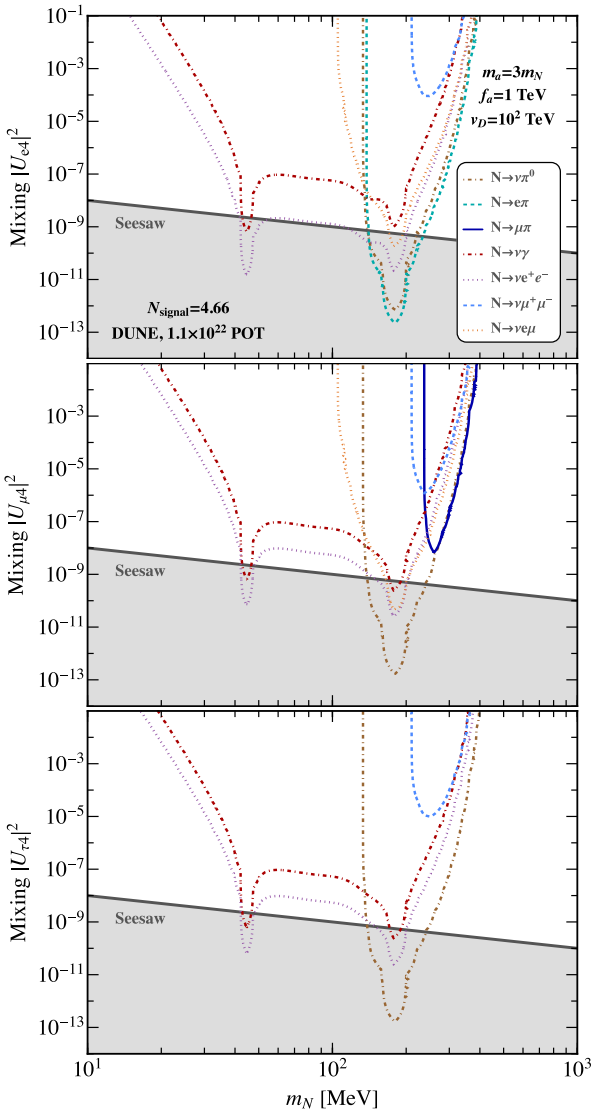

FIG. 4. The sensitivity of the DUNE near detector to the HNLs produced from the dark pion decay, assuming a total of 1.1×10^{22} POT. The panels correspond to different HNL mixing structures, namely, mixing only with ν_e (top), ν_μ (middle), and ν_τ (bottom), respectively.

naturally agree with expectation from the naive type-I seesaw. These regions of parameter space are highlighted in gray in Fig. 4 and correspond to $|U_{\alpha 4}|^2 \leq 0.1$ eV$/m_N$ [28].

Conclusion—SM-singlet fermions are often among the ingredients behind nonzero neutrino masses. If this is the case, and if these new particles are light enough, they can be produced and detected in fixed-target-like experiments, like the DUNE near-detector facility. Here, we explore the fact that the production and detection of SM-singlet fermions are model dependent. We show that, if these belong to a richer—but rather generic—dark sector, it is possible that an experiment like DUNE can explore regions of parameter space relevant for the neutrino mass puzzle.

In more detail, after electroweak symmetry breaking, SM-singlet fermions, also referred to as HNLs, naturally mix with SM neutrinos. If these are light enough, they can be produced via the weak interactions in the decay of charged mesons (e.g., $\pi^+ \to \mu^+ N$) and decay via the weak interactions into leptons and other light states. On the other hand, ALPs will naturally decay, often with large branching ratio, into HNLs if these belong to the same dark sector. Since ALPs mix with the SM neutral pseudoscalar hadrons, we explored for the first time the consequences of the fact that the HNL flux at a fixed-target-like facility might be predominantly associated with the production of neutral mesons, including the π^0 and the η. If this is the case, the physics responsible for HNL production and decay is not directly related and the production rate is not suppressed by the active-sterile mixing parameters. Furthermore, experiments like DUNE might be sensitive to HNLs that are too weakly coupled, directly, to the SM to be produced in the decay of charged mesons. This is naively expected, for example, of HNLs that play a direct part in the type-I seesaw mechanism.

Our analyses are confined to the DUNE experiment, but we anticipate that the HNL-ALP connection will lead to interesting consequences across the spectrum of neutrino facilities, including ICARUS, SBND, μBooNE, COHERENT, CCM, and FASERν and provide a new avenue for future research and experimentation in the quest to uncover the mysteries of HNLs and their role in particle physics.

Acknowledgments—The work of A. d. G is supported in part by the U.S. Department of Energy Grant No. DE-SC0010143 and in part by the NSF Grant No. PHY-1630782. The work of B. D. is supported by the U.S. Department of Energy Grant No. DE-SC0010813. The work of Z. T. is supported by the Neutrino Theory Network Program Grant No. DE-AC02-07CHI11359 and the U.S. Department of Energy under the Award No. DE-SC0020250. She also appreciates the hospitality of Aspen Physics Center where this work was partially developed. The work of I. M. S. is supported by the U.S. Department of Energy Grant No. DE-SC0020262. A. A. acknowledges partial support from the European Union's Horizon 2020 research and innovation program under the Marie Sklodowska-Curie Grant Agreement No. 860881-HIDDeN and the Marie Sklodowska-Curie Staff Exchange Grant Agreement No. 101086085–ASYMMETRY; from Fermi National Accelerator Laboratory, managed and operated by Fermi Research Alliance, LLC under Contract No. DE-AC02-07CH11359 with the U.S. Department of Energy; and from the Spanish Research Agency (Agencia Estatal de Investigación) through the Grant IFT Centro de Excelencia Severo Ochoa No. CEX2020-001007-S and the Grant No. RYC2018-024240-I, funded by MCIN/AEI/10.13039/501100011033 and by "ESF Investing in your future".

[1] Y. Fukuda *et al.* (Super-Kamiokande Collaboration), Phys. Rev. Lett. **81**, 1562 (1998).
[2] Y. Fukuda *et al.* (Super-Kamiokande Collaboration), Phys. Rev. Lett. **82**, 2644 (1999).
[3] Q. R. Ahmad *et al.* (SNO Collaboration), Phys. Rev. Lett. **89**, 011301 (2002).
[4] P. Minkowski, Phys. Lett. **67B**, 421 (1977).
[5] R. N. Mohapatra and G. Senjanovic, Phys. Rev. Lett. **44**, 912 (1980).
[6] M. Gell-Mann, P. Ramond, and R. Slansky, Conf. Proc. C **790927**, 315 (1979).
[7] T. Yanagida, Conf. Proc. C **7902131**, 95 (1979).
[8] G. Lazarides, Q. Shafi, and C. Wetterich, Nucl. Phys. **B181**, 287 (1981).
[9] R. N. Mohapatra and G. Senjanovic, Phys. Rev. D **23**, 165 (1981).
[10] J. Schechter and J. W. F. Valle, Phys. Rev. D **22**, 2227 (1980).
[11] T. P. Cheng and L.-F. Li, Phys. Rev. D **22**, 2860 (1980).
[12] R. Foot, H. Lew, X. G. He, and G. C. Joshi, Z. Phys. C **44**, 441 (1989).
[13] W. Konetschny and W. Kummer, Phys. Lett. **70B**, 433 (1977).
[14] E. Ma, Phys. Rev. Lett. **81**, 1171 (1998).
[15] B. Bajc and G. Senjanovic, J. High Energy Phys. 08 (2007) 014.
[16] I. Dorsner and P. Fileviez Perez, J. High Energy Phys. 06 (2007) 029.
[17] C. Boehm and P. Fayet, Nucl. Phys. **B683**, 219 (2004).
[18] C. Boehm, P. Fayet, and J. Silk, Phys. Rev. D **69**, 101302(R) (2004).
[19] M. Pospelov, A. Ritz, and M. B. Voloshin, Phys. Lett. B **662**, 53 (2008).
[20] M. Pospelov, Phys. Rev. D **80**, 095002 (2009).
[21] M. Fukugita and T. Yanagida, Phys. Lett. B **174**, 45 (1986).
[22] S. Davidson, E. Nardi, and Y. Nir, Phys. Rep. **466**, 105 (2008).
[23] A. Atre, T. Han, S. Pascoli, and B. Zhang, J. High Energy Phys. 05 (2009) 030.
[24] R. Essig *et al.*, arXiv:1311.0029.
[25] M. Drewes, Int. J. Mod. Phys. E **22**, 1330019 (2013).
[26] K. Bondarenko, A. Boyarsky, and N. Medvedko, J. High Energy Phys. 01 (2018) 021.
[27] J. Beacham *et al.*, J. Phys. G **47**, 010501 (2020).
[28] P. Ballett, T. Boschi, and S. Pascoli, J. High Energy Phys. 03 (2020) 111.
[29] J. Berryman *et al.*, J. High Energy Phys. 02 (2020) 174.
[30] M. Pospelov, Phys. Rev. D **84**, 085008 (2011).
[31] R. Harnik, J. Kopp, and P. A. N. Machado, J. Cosmol. Astropart. Phys. 07 (2012) 026.
[32] B. Batell, M. Pospelov, and B. Shuve, J. High Energy Phys. 08 (2016) 052.
[33] Y. Farzan and J. Heeck, Phys. Rev. D **94**, 053010(2016).
[34] V. De Romeri, E. Fernandez-Martinez, J. Gehrlein, P. A. N. Machado, and V. Niro, J. High Energy Phys. 10 (2017) 169.
[35] G. Magill, R. Plestid, M. Pospelov, and Y.-D. Tsai, Phys. Rev. D **98**, 115015 (2018).
[36] E. Bertuzzo, S. Jana, P. A. N. Machado, and R. Zukanovich Funchal, Phys. Lett. B **791**, 210 (2019).
[37] E. Bertuzzo, S. Jana, P. A. N. Machado, and R. Zukanovich Funchal, Phys. Rev. Lett. **121**, 241801 (2018).
[38] P. Ballett, M. Hostert, and S. Pascoli, Phys. Rev. D **99**, 091701(R) (2019).
[39] P. Ballett, M. Hostert, and S. Pascoli, Phys. Rev. D **101**, 115025 (2020).
[40] P. Coloma, Eur. Phys. J. C **79**, 748 (2019).
[41] O. Fischer, A. Hernández-Cabezudo, and T. Schwetz, Phys. Rev. D **101**, 075045 (2020).
[42] J. M. Cline, M. Puel, and T. Toma, J. High Energy Phys. 05 (2020) 039.
[43] M. Berbig, S. Jana, and A. Trautner, Phys. Rev. D **102**, 115008 (2020).
[44] A. M. Abdullahi *et al.*, J. Phys. G **50**, 020501 (2023).
[45] J. M. Berryman, A. de Gouvêa, K. J. Kelly, and Y. Zhang, Phys. Rev. D **96**, 075010 (2017).
[46] A. de Giorgi, L. Merlo, and J.-L. Tastet, Fortschr. Phys. **71**, 2300027 (2023).
[47] A. Alves, A. G. Dias, and D. D. Lopes, J. High Energy Phys. 08 (2020) 074.
[48] J. Bonilla, B. Gavela, and J. Machado-Rodríguez, Phys. Rev. D **109**, 055023 (2024).
[49] L. M. Krauss and M. B. Wise, Phys. Lett. B **176**, 483 (1986).
[50] D. S. M. Alves and N. Weiner, J. High Energy Phys. 07 (2018) 092.
[51] W. Altmannshofer, S. Gori, and D. J. Robinson, Phys. Rev. D **101**, 075002 (2020).
[52] K. J. Kelly, S. Kumar, and Z. Liu, Phys. Rev. D **103**, 095002 (2021).
[53] V. Brdar, B. Dutta, W. Jang, D. Kim, I. M. Shoemaker, Z. Tabrizi, A. Thompson, and J. Yu, Phys. Rev. Lett. **126**, 201801 (2021).
[54] V. Brdar, B. Dutta, W. Jang, D. Kim, I. M. Shoemaker, Z. Tabrizi, A. Thompson, and J. Yu, Phys. Rev. D **107**, 055043 (2023).
[55] S. Agostinelli *et al.* (GEANT4 Collaboration), Nucl. Instrum. Methods Phys. Res., Sect. A **506**, 250 (2003).
[56] B. Abi *et al.* (DUNE Collaboration), arXiv:2002.03005.
[57] P. B. Pal and L. Wolfenstein, Phys. Rev. D **25**, 766 (1982).
[58] D. Gorbunov and M. Shaposhnikov, J. High Energy Phys. 10 (2007) 015; 11 (2013) 101(E).
[59] J. Conrad, A. de Gouvea, S. Shalgar, and J. Spitz, Phys. Rev. D **82**, 093012 (2010).
[60] A. de Gouvêa, K. J. Kelly, G. V. Stenico, and P. Pasquini, Phys. Rev. D **100**, 016004 (2019).
[61] P. Machado, H. Schulz, and J. Turner, Phys. Rev. D **102**, 053010 (2020).
[62] P. S. B. Dev, B. Dutta, T. Han, and D. Kim, Phys. Lett. B **850**, 138500 (2024).
[63] S. A. Meighen-Berger, J. F. Beacom, N. F. Bell, and M. J. Dolan, Phys. Rev. D **109**, 092006 (2024).
[64] R. Mammen Abraham *et al.*, J. Phys. G **49**, 110501 (2022).

End Matter

Appendix—For the expressions of the partial HNL decay widths we have used the expressions in Appendix A of [45], as well as Refs. [28,57,58]. In general, with all the decay channels that are kinetically allowed for the mass range we consider in this Letter, the total decay width reads

$$\Gamma_N^{\rm Total} = 2\sum_{\alpha=e,\mu,\tau}\Big[\Gamma(N\to\nu_\alpha\bar{\nu}\nu)+\Gamma(N\to\nu_\alpha\gamma)+\Gamma(N\to\nu_\alpha\pi^0)\Big] + 2\sum_{\alpha=e,\mu}\Big[\Gamma(N\to\pi^+\ell_\alpha)+\Gamma(N\to\ell_\alpha^-\ell^+\nu) + \Gamma(N\to\ell_\alpha^-\ell^+\nu)+\Gamma(N\to\nu_\alpha\ell^-\ell^+)\Big], \tag{A1}$$

where the overall factor of 2 accounts for the fact that the HNLs are Majorana fermions. We have shown the branching fractions in Fig. 5, where we have assumed all the mixing angles $|U_{\alpha 4}|^2$ are equal and can be canceled from the expressions of the branching fractions.

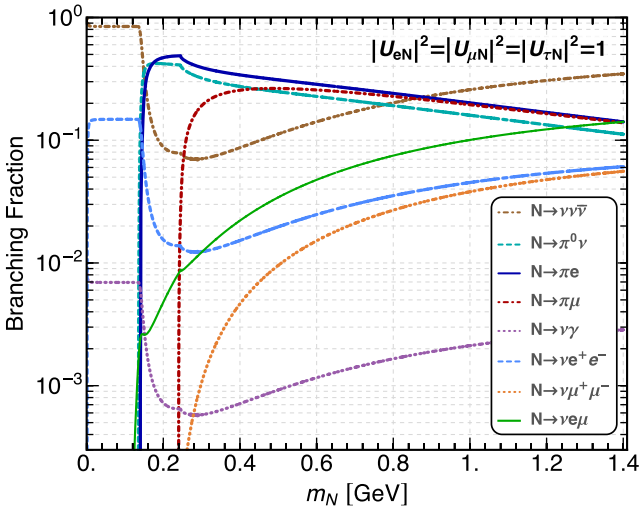

FIG. 5. Branching fractions for different decay modes of the HNL, as a function of the HNL mass m_N.

To demonstrate the dependence of our final results on the value of the dark vacuum expectation value v_D, we have made Fig. 6, for which all the parameters are the same as in Fig. 4, but $v_D = 10^3$ TeV.

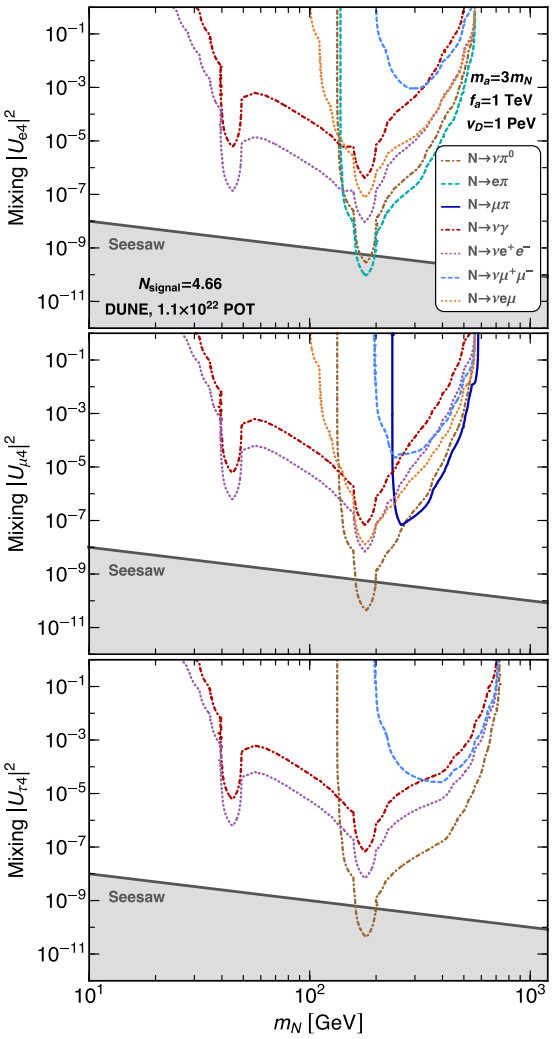

FIG. 6. Same as Fig. 4, for $v_D = 10^3$ TeV.